frontiers in Toxicology

TYPE Original Research
PUBLISHED 10 November 2026
DOI 10.3389/ftox.2026.1963820

Check for updates

OPEN ACCESS

EDITED BY
Todd Stueckle,
US Army Medical Research Institute of Chemical Defense, United States

REVIEWED BY
Suresh Kumar Kolli,
Gandhi Institute of Technology and Management (GITAM), India
ALPER YARDAN,
Balıkesir University, Türkiye

*CORRESPONDENCE
Ulla Vogel,
ubv@nfa.dk

RECEIVED 10 August 2026
REVISED 11 September 2026
ACCEPTED 01 October 2026
PUBLISHED 10 November 2026

CITATION
Danielsen PH, Hedmer M, Abrahamsson C, Berthing T, Sundberg M, Sørli JB, Kåredal M, Lei P, Erdem JS, Yang G, Rehberg M, Isaxon C and Vogel U (2026) Occupational exposure to cement dust and potential pulmonary and systemic effects.
Front. Toxicol. 8:1963820.
doi: 10.3389/ftox.2026.1963820

COPYRIGHT
© 2026 Danielsen, Hedmer, Abrahamsson, Berthing, Sundberg, Sørli, Kåredal, Lei, Erdem, Yang, Rehberg, Isaxon and Vogel. This is an open-access article distributed under the terms of the Creative Commons Attribution License (CC BY). The use, distribution or reproduction in other forums is permitted, provided the original author(s) and the copyright owner(s) are credited and that the original publication in this journal is cited, in accordance with accepted academic practice. No use, distribution or reproduction is permitted which does not comply with these terms.

Occupational exposure to cement dust and potential pulmonary and systemic effects

Pernille Høgh Danielsen[1], Maria Hedmer[2,3,4], Camilla Abrahamsson[5], Trine Berthing[1], Mathilde Sundberg[1], Jorid Birkelund Sørli[1], Monica Kåredal[2,3,4], Peng Lei[6], Johanna Samulin Erdem[6], Guo Yang[7], Markus Rehberg[7], Christina Isaxon[4,5] and Ulla Vogel[1,8]*

[1]National Research Centre for the Working Environment (NFA), Copenhagen, Denmark, [2]Department of Occupational and Environmental Medicine, Skåne University Hospital, Lund, Sweden, [3]Division of Occupational and Environmental Medicine, Department of Laboratory Medicine, Lund University, Lund, Sweden, [4]NanoLund, Lund University, Lund, Sweden, [5]Ergonomics and Aerosol Technology, Department of Design Sciences, Faculty of Engineering, Lund University, Lund, Sweden, [6]National Institute of Occupational Health, Oslo, Norway, [7]Institute of Lung Health and Immunity (LHI), Comprehensive Pneumology Center (CPC), Helmholtz Center Munich, Member of the German Center for Lung Research (DZL), Munich, Germany, [8]National Food Institute, Technical University of Denmark, KgsLyngby, Denmark

Introduction: Cement production is a major source of occupational exposure to airborne particles, yet detailed characterization of exposure and associated health effects remains limited.
Methods: Emissions and worker exposures were assessed during clinker mineral production, cement grinding, and bagging using filter-based sampling and direct-reading instruments. The pulmonary toxicity of collected PM2.5 (particulate matter with an aerodynamic diameter <2.5 μm) was evaluated using both an in vitro model and in vivo mouse models.
Results: Personal full-shift measurements showed average exposures to inhalable and respirable dust of 2.2 mg/m^3 and 0.058 mg/m^3, respectively. Time-resolved measurements demonstrated exposure to particles <300 nm, with a mean particle number concentration of 13,800 cm^{-3} and a lung-deposited surface area concentration of 40 μm^2/cm^3. Most particles, by number concentration, were 50–60 nm. Calcium was the dominant constituent, with contributions from iron, aluminum, and magnesium. To assess potential health effects, PM2.5 samples from clinker production and cement bagging were administered to mice by intratracheal instillation, and responses were evaluated at 1, 3, and 28 days post-exposure. Both materials induced mild pulmonary responses, with no marked cytotoxicity or tissue injury. Clinker PM2.5 elicited slightly stronger effects than cement PM2.5, including modest increases in bronchoalveolar lavage cell counts and macrophages at the latest time point, and an early pulmonary acute phase response. Intravital lung microscopy revealed rapid neutrophil recruitment following clinker PM2.5 exposure, indicating an early innate immune response.
Conclusion: The findings demonstrate that cement production workers were exposed to low levels of respirable particles. The collected PM2.5 samples induced mild pulmonary responses in vivo, with slight differences between particles from the clinker production and cement bagging sites.

KEYWORDS
cement dust, inflammation, neutrophil influx, personal exposure assessment, respirable, particles, serum amyloid A

1 Introduction

Cement production begins with a mixture of crushed limestone, sand and clay which is heated to approximately 1,500 °C in a rotating kiln. This process produces solid clumps known as clinker. The clinker is subsequently cooled and milled into a fine powder, which is mixed with gypsum to produce cement (Aranda-Usón et al., 2013). During the production and handling of cement, various processes can generate airborne particulate matter (PM), resulting in occupational dust exposure among workers. Cement dust is a complex mixture of calcium oxide, silica, aluminum compounds, iron oxides, and various trace elements (Fell and Nordby, 2017), often containing respirable particles (Notø et al., 2016). Occupational exposure to cement dust is therefore an important health concern in the cement industry.

Epidemiological studies report increased respiratory symptoms among cement production workers, including cough, wheezing, and dyspnea (Fell and Nordby, 2017). Cross-sectional studies show reduced lung function at exposure levels ≥4.5 mg/m^3 of total dust and 2.3 mg/m^3 of respirable dust (Fell and Nordby, 2017). Longitudinal studies link cement dust exposure and declining lung function, with estimated lowest effect levels of 0.8–1.1 mg/m^3 for respirable dust, 3.7–5.4 mg/m^3 for total dust, and 9.2–13 mg/m^3 for inhalable dust (Nordby et al., 2016). The alkalinity of cement components, particularly clinker, may cause mucosal irritation and inflammation, potentially leading to chronic bronchitis and obstructive lung disease (Weinbruch et al., 2023).

Some studies suggest systemic responses to cement dust exposure, including altered circulating inflammatory markers such as fibrinogen and cytokines (Fell et al., 2011), as well as increased neutrophils and IL-1β in sputum from exposed workers (Fell et al., 2010). Exposure among cement workers has been investigated using filter-based sampling methods to determine airborne dust fractions (Fell and Nordby, 2017). Cement composition and production processes have evolved over time, including the use of additives and finer grinding, which may influence exposure characteristics and potential health effects (Notø, 2019).

Particle number concentration (PNC) and lung-deposited surface area (LDSA) are increasingly used to characterize occupational exposure to ultrafine particles (Hedmer et al., 2026; Hedmer et al., 2017; Isaxon et al., 2020; Loven et al., 2021; Loven et al., 2024). However, time-resolved personal exposure studies in cement production are scarce, and no *in vivo* studies have used airborne material collected from cement production. The aim of this study was therefore to characterize time-resolved occupational exposure to coarse and ultrafine particles during different stages of cement production and to evaluate the pulmonary toxicity of collected PM2.5 (particulate matter with aerodynamic diameter <2.5 μm) using both an *in vitro* model and *in vivo* mouse models.

2 Methods

2.1 Personal exposure measurements

Full-shift airborne dust exposure was measured over two consecutive days in the personal breathing zones (PBZ) of ten non-smoking male production workers at a larger Central European cement plant. Six workers performed multiple tasks, including quarry monitoring, raw meal grinding, additive handling, and cement grinding (Table 1). These workers partly used respiratory protection during dusty tasks. One worker primarily worked outdoors handling fuels used for heating different production processes. Three workers monitored automatic cement bagging into 25-kg bags. The bagging system was partly enclosed and equipped with process ventilation. Two workers did not use respiratory protection during bagging, whereas one used it intermittently.

2.2 Real-time particle measurements

Three portable monitors (Partector 2, Naneos, Windisch, Switzerland) measured PNC, LDSA, PM0.3, and mean particle size (10–300 nm) with 1 s time resolution. The monitors were deployed on six workers; due to instrumental failure, valid data were obtained from five. Sampling inlets were positioned in the PBZ (collarbone). Two monitors were fitted with a respirable dust cyclone (GS3, SKC Inc., Eighty Four, PA, United States) to remove coarse particles.

2.3 Sampling of inhalable and respirable dust

Inhalable dust was collected on 25-mm polytetrafluoroethylene (PTFE) filters mounted in IOM filter cassettes using Apex2 pumps (Casella, Bedford, United Kingdom) at 2.0 L min^{-1} in the PBZ and near-field stationary samples (~1 m from the bagging process).

Respirable dust was collected on 37-mm PTFE filters mounted in conductive open-face three-piece cassettes (SureSeal, SKC Inc., Eighty Four, PA, United States) fitted with BGI4L cyclones (BGI Inc., Waltham, MA, United States; 4-μm cutoff at 2.2 L min^{-1}). For inhalable dust we had five field blanks and for respirable dust, we had three field blanks. Sampling durations ranged from 412 to 463 min.

2.4 Stationary sampling of airborne particles

PM2.5 was collected at two locations in the cement production plant: (1) a corridor where clinker clumps were transported by conveyor belt from the calcination kiln for cooling, and (2) the cement bagging area. Instruments were positioned 1–3 m from emission sources (Supplementary Figure S1). Three PM2.5 field blanks were brought to the collection sites.

PNC (20 nm–1 μm) were measured using a P-Trak (model 8525, TSI Inc., Shoreview, MN, United States) with 60-s time resolution. Particle number size distributions (14.3–723 nm) were measured using a scanning mobility particle sizer (SMPS; differential mobility analyzer (DMA) 3082, condensation particle counter (CPC) 3772, TSI Inc., Shoreview, MN, United States) with a 120 s scan time. Particles in the 0.5–20 μm size range were measured using an aerodynamic particle sizer (APS; model 3321, TSI Inc., Shoreview, MN, United States) with 20 s time resolution. Relative mass concentrations of PM1, PM2.5, the respirable fraction, PM10, and total dust were measured using a DustTrak (DRX 8534, TSI Inc., Shoreview, MN, United States) with 60 s time resolution.

PM2.5 was collected on PTFE membrane filters (TE38, Whatman, Maidstone, United Kingdom) using a high-volume sampler (BGI900, BGI Inc., Waltham, MA, United States)

TABLE 1 Personal exposure to dust measured as inhalable and respirable dust fractions.

Worker no.	Work task	Use of respiratory protection	Sampling time (min)	Inhalable dust (mg/m^3)	Respirable dust (mg/m^3)	Ratio respirable/ Inhalable dust
Clinker and cement production						
1	Working with raw material and cement production	FFP3 during 4 h	447	13	0.081	0.0062
2	Working with raw material production	FFP3 during 4 h	450	2.7	<LOD*	0.0093
3	Working with raw material production	FFP3 most of the day	446	1.1	<LOD*	0.023
4	Working with cement production	Partly, during work in the mill	459	4.8	0.27	0.056
5	Working with cement production	Partly, during work in the mill	456	1.3	0.12	0.092
6	Working with cement production	FFP3 during 6 h	446	3.4	<LOD*	0.0074
Packaging of cement						
7	Bagging of dry cement	None	424	1.8	<LOD*	0.015
8	Bagging of dry cement	FFP3 during 0.5 h	414	3.6	0.22	0.061
9	Bagging of dry cement	None	412	1.6	0.066	0.041
Other work tasks						
10	Working with fuels	FFP3 during 0.5 h	463	0.4	<LOD*	0.063
*EU-OEL***				*5.0–10*	*2.5–5*	

*The value was below limit of detection. **Based on Danish and Swedish OELs. FFP3, filtering facepiece class 3; LOD, limit of detection; EU-OEL, european occupational exposure limit.

operated at 900 L min^{-1}. The sampler was positioned 1.5 m above ground. Filters, including blanks, were weighted before and after sampling. Collected PM2.5 was extracted in analytical-grade methanol, dried under nitrogen, and stored for subsequent analyses and *in vivo* experiments. The samples are referred to as Cement PM2.5 and Clinker PM2.5.

2.5 Gravimetric analysis

Gravimetric analysis was performed using an analytical balance (XP105 DR, Mettler Toledo, Greifensee, Switzerland). Limits of detection (LOD) were 0.05 mg/sample for respirable dust and PM2.5, and 0.1 mg/sample for inhalable dust.

2.6 Elemental particle analysis

Element concentrations were determined by inductively coupled plasma mass spectrometry (ICP-MS; Thermo iCAP TQe, Thermo Fischer Scientific, Waltham, MA, United States) equipped with an Elemental Scientific 4DX autosampler. Analysis used kinetic energy discrimination with helium collision gas. Filters were dissolved overnight in 1 mL concentrated nitric acid at 70 °C. 9 mL ultrapure water was added, and the solutions were transferred to acid-washed polypropylene tubes. Stock solutions were diluted 1:10, 1:100, or 1:500 in 2% nitric acid to 5 mL. Rhodium, scandium, and terbium were added as internal standards. Calibration standards were prepared from a 10 ppm multi-element ICP-MS standard (ICP-MS-CAL2-1, AccuStandard, New Haven, CT, United States). Limits of quantification were defined as 10 times the standard deviation of field blank signals. Clinker PM2.5, Cement PM2.5, respirable dust, and inhalable dust were analyzed.

Additionally, samples of clinker and cement dust were analyzed for the chemical form of their iron (Fe) content by synchrotron X-ray absorption spectroscopy. Scans were taken at 2–3 different positions in each sample using both fluorescence mode with a passivated implanted planar silicon (PIPS) diode and transmission mode. Obtained spectra were compared to reference spectra of relevant Fe-containing minerals.

2.7 Preparation of *in vivo* instillation suspensions

Cement PM2.5 and Clinker PM2.5 were dispersed at 3.24 mg/mL in Nanopure water containing 2% mouse serum and probe-

sonicated on ice for 16 min using a Branson Sonifier S-450D (Branson Ultrasonics Corp., Danbury, CT, United States) as previously described (Danielsen et al., 2020; Jackson et al., 2011).

The stock suspension (162 μg/50 μL) was diluted to 1.08 and 0.36 mg/mL, yielding doses of 54 and 18 μg/50 μL, respectively. Diluted suspensions were probe-sonicated for an additional 4 min.

Printex90 carbon black particles were included as reference material (162 μg/mouse), and vehicle control mice were administered Nanopure water containing 2% mouse serum. Instillations were performed with a volume of 50 μL/mouse.

Particle size distribution and polydispersity were determined by dynamic light scattering (DLS; Malvern Nano Zetasizer, Malvern Instruments Ltd., Malvern, United Kingdom) based on six repeated measurements.

2.8 Microbial contamination

Endotoxin content in Cement and Clinker PM2.5 was quantified using the Limulus Amebocyte Lysate (LAL) assay (Kinetic-QCL™, Lonza, Walkersville, MD, United States). Particle suspensions were prepared in endotoxin-free water (LAL Reagent Water, Lonza, Walkersville, MD, United States) at 0.6 mg/mL and 1.1 mg/mL, respectively. Endotoxin was quantified from a standard curve prepared from serial dilutions of control standard endotoxin (*Escherichia coli* O55:B5; Lonza, Walkersville, MD, United States) and normalized to particle mass as endotoxin units (EU)/mg. Inhibition–enhancement controls verified the absence of particle-induced assay interference (spike recovery 50%–200%). The LOD was 0.005 EU/mL.

To assess microbial contaminants beyond endotoxin, Cement PM2.5 and Clinker PM2.5 were evaluated in the HEK-Blue™ hTLR2 and HEK-Blue™ hTLR4 reporter cell assays (InvivoGen, Toulouse, France) (Lei et al., 2025). Cells were seeded at 280,000 cells/mL in 96-well plates overnight. Cement PM2.5 and Clinker PM2.5 were probe-sonicated in 0.05% (v/v) bovine serum albumin (BSA) in endotoxin-free water (16 min; Branson Sonifier S-450D) and added to the cells at 100 μg/mL for 24 h. Ultrapure lipopolysaccharide (LPS) from *E. coli* (*E. coli* O55:B5), (tlrl-b5lps, InvivoGen, Toulouse, France) and lipoteichoic acid (LTA) from *Staphylococcus aureus* (tlrl-pslta, InvivoGen, Toulouse, France) served as positive controls, while endotoxin-free water served as negative control. Secreted embryonic alkaline phosphatase (SEAP) activity was measured by transferring 20 μL supernatant to 180 μL QUANTI-Blue™ Solution (InvivoGen, Toulouse, France), incubating for 3 h at 37 °C, and measuring absorbance at 649 nm using a Synergy Neo2 plate reader (BioTek Instruments, Winooski, VT, United States). Data are presented as fold-change relative to untreated cells.

2.9 Animals and exposure

A total of 159 seven-week-old female C57BL/6JRj mice (Janvier Labs, Le Genest-Saint-Isle, France) were randomly assigned to exposure groups and housed under standard conditions with *ad libitum* access to food and water as previously described (Hadrup et al., 2017).

Mice were anesthetized by inhalation of 4% isoflurane and exposed to 50 μL Clinker PM2.5, Cement PM2.5, Printex90, or vehicle by a single intratracheal instillation (Hadrup et al., 2025; Jackson et al., 2011; Saber et al., 2012a) and terminated at 1, 3, and 28 days post-exposure. Lung toxicity was assessed in groups of six mice per dose level. Separate groups (n = 5) receiving 162 μg/mouse were used for biopersistence at 28 days post-exposure. Each exposure series included vehicle controls, resulting in 12 control animals per time point.

2.10 Collection of bronchoalveolar lavage and tissues

Mice were euthanized by intraperitoneal injection of Zoletil Forte (250 mg/mL), Rompun (20 mg/mL), and Fentanyl (50 μg/mL) in sterile saline (0.1 mL/10 g body weight) in combination with heart blood withdrawal. Bronchoalveolar lavage (BAL) fluid was collected by flushing the lungs twice with 1 mL sterile saline and centrifuged (400 x g, 10 min, 4 °C) to separate cells from supernatant. BAL supernatants were used for tgaotal protein and lactate dehydrogenase (LDH) analyses. Lung and liver tissues were snap-frozen in liquid nitrogen and stored at −80 °C until RNA isolation.

2.11 Cell viability and differential cell counts

Cell pellets from BAL were resuspended in HAM F-12 medium supplemented with 10% fetal bovine serum. Total BAL cell counts and viability were determined using a NucleoCounter NC-200 (Chemometec, Allerød, Denmark). Differential cell counts were performed as previously described by Danielsen et al. (2021). Briefly, BAL cells were cytocentrifuged onto microscope slides, fixed, and stained with May–Grünwald–Giemsa. Macrophages, neutrophils, lymphocytes, and eosinophils were distinguished based on their characteristic morphology and staining properties. Slides were blinded prior to manual differential counting, and 200 cells per sample were evaluated.

2.12 Total protein and LDH in BAL supernatant

Total protein in BAL supernatants was quantified using the Pierce™ BCA Protein Assay Kit (Thermo Fisher Scientific, Waltham, MA, United States) as previously described (Danielsen et al., 2025). LDH activity was measured using the Lactate Dehydrogenase Assay Kit (Abcam, Cambridge, United Kingdom). For each individual animal, measurements were performed in technical duplicate.

2.13 Gene expression of *Saa3* in lung tissue and *Saa1* in liver tissue

Total RNA was isolated using the QIAwave RNA Plus Mini Kit (QIAGEN, Hilden, Germany; Cat. No. 74104) according to the manufacturer's instructions, including genomic DNA removal using the gDNA Eliminator spin column. No additional DNase treatment was performed. All RNA handling was performed using certified RNase- and DNase-free plasticware and nuclease-free water, with gloves worn throughout sample handling. RNA concentrations and purity were measured using a NanoDrop 2000c spectrophotometer

(Thermo Fisher Scientific, Waltham, MA, United States). RNA purity was considered acceptable when A260/A280 and A260/A230 ratios were within 1.8–2.2. Complementary DNA (cDNA) was synthesized using TaqMan® Reverse Transcription Reagents (Applied Biosystems, Foster City, CA, United States) according to the manufacturer's instructions.

Gene expression was quantified by reverse-transcriptase quantitative polymerase chain reaction (RT-qPCR) as previously described (Saber et al., 2009; Poulsen et al., 2017). *Saa1* expression was measured using the predesigned TaqMan™ Gene Expression Assay Mm00656927_g1 (Applied Biosystems, Foster City, CA, United States), which includes gene-specific primers and a FAM-labeled TaqMan probe. *Saa3* expression was analyzed using custom primers (forward: 5′-GCC TGG GCT GCT AAA GTC AT-3′; reverse: 5′-TGC TCC ATG TCC CGT GAA C-3′) synthesized by TAG Copenhagen A/S (Copenhagen, Denmark), together with a custom TaqMan™ TAMRA probe (5′-FAM-TCT GAA CAG CCT CTC TGG CAT CGC T-TAMRA-3′; Cat. No. 450025; Applied Biosystems, Foster City, CA, United States of America). Eukaryotic 18S ribosomal RNA (rRNA) served as the endogenous control (Applied Biosystems, Foster City, CA, United States). Samples from each individual animal were analyzed in technical triplicate using a ViiA7 Real-Time PCR detector (Applied Biosystems, Foster City, CA, United States). Negative controls were included in each run, and relative gene expression was calculated using the comparative Ct method.

2.14 Biopersistence in mouse lung tissue

Biopersistence was qualitative assessed by enhanced darkfield microscopy (Berthing et al., 2023). At 28 days post-exposure, lungs from mice exposed to 162 µg/mouse and vehicle controls were inflation-fixed with 4% formalin, immersed in formalin for 24 h, embedded in paraffin, sectioned at 2–3 µm, and stained with eosin. One longitudinal section from the left lung lobe of three mice per group was partially scanned at 40x using enhanced darkfield microscopy (CytoViva, Auburn, AL, United States). Images were acquired at 100x magnification using a Qimaging Retiga4000R camera.

2.15 Lung intravital microscopy (L-IVM)

Lung intravital microscopy (L-IVM) was performed as previously described (Li et al., 2024; Liu et al., 2025) in a dedicated subset of mice (n = 3 per group) assigned to the vehicle and Clinker PM2.5 groups. L-IVM was not performed with Cement PM2.5 because of limited material.

Ten-week-old female C57BL/6 mice (Charles River, Sulzfeld, Germany) were anesthetized by intraperitoneal injection of medetomidine (0.5 mg/kg), midazolam (5 mg/kg), and fentanyl (0.05 mg/kg) (MMF), maintained at 37 °C, and continuously monitored (Harvard Apparatus, Holliston, MA, United States). The neck and left chest were locally anesthetized with Bucaine (50 µg/site, Puren Pharma GmbH & Co. KG, Munich, Germany). Anesthesia was maintained by administration of half the initial MMF dose every 45 min.

Following induction of anesthesia, neutrophils were labeled *in vivo* by intravenous injection of 6 µg Alexa Fluor® 488-conjugated anti-mouse Ly6G antibody in Dulbecco's phosphate buffered saline (clone 1A8, BioLegend, San Diego, CA, United States) 15 min before imaging.

Following tracheostomy, a blunt 20G catheter (B. Braun, Melsungen, Germany) was inserted <5 mm into the trachea and connected to a rodent ventilator (MiniVent, Harvard Apparatus, Holliston, MA, United States). Mice were ventilated with 100% oxygen at a tidal volume of 10 µL/g body weight, 100 breaths/min, and a positive end-expiratory pressure (PEEP) of 0.1 cm/g body weight.

Mice were placed in right lateral decubitus position, and a custom-made flanged thoracic suction window was inserted into a 5-mm intercostal incision between ribs three and four of the left chest. The lung was immobilized using 20–25 mmHg negative pressure generated by a custom-made system comprising a differential pressure gauge (Magnehelic, Dwyer Instruments, Inc., Michigan City, IN, United States) and a negative pressure pump (Nupro, Willoughby, OH, United States).

Imaging was performed using a VisiScope A1 microscope (Visitron Systems GmbH, Puchheim, Germany) equipped with a CoolLed p-4000 fluorescence light source (Andover, United Kingdom). Anti-Ly6G-488 was exicted at 490 nm (50% power, 80 m exposure). Fluorescence was directed through a quad-band filter (F66-014, DAPI/FITC/Cy3/Cy5 Quad LED ET Set; AHF Analysentechnik AG, Tübingen, Germany). Images were acquired using a 20x water-dipping objective (NA 1.0; Zeiss MicroImaging GmbH, Jena, Germany), a T 580 lpxxr beam splitter (Chroma Technology Corp, Bellows Falls, VT, United States), two Rolera EM2 cameras, and VisiView Imaging software (Visitron Systems GmbH, Puchheim, Germany).

After baseline imaging (t = 0), Clinker PM2.5 (162 µg/50 µL) was instilled through the tracheal catheter while ventilation was briefly disconnected. Mice were then placed upright for 5 min to facilitate particle distribution. During this period, ventilator settings were adjusted to a tidal volume of 15 µL/g body weight, 150 breaths/minute, a PEEP of 0.1 cm/g body weight, and 100% oxygen.

To quantify neutrophil recruitment after exposure, five regions of interest were recorded at 0, 30, 60, and 90 min, and 15-s image sequences were analyzed using ImageJ software (National Institutes of Health, Bethesda, MD, United States). Neutrophils were automatically counted using the Trackmate function of ImageJ, with the baseline image used to define the detection threshold. The same settings were applied throughout, and counts were manually corrected.

The mice were euthanized immediately after completion of the final 90-min imaging time point using an overdose of anaesthetic (0.800 mg/g Ketabel and 0.0088 mg/g Xylazine).

2.16 Inhibition of lung surfactant (LS) function *in vitro*

The effect of Clinker and Cement PM2.5 on LS function was measured using a constrained drop surfactometer (CDS) (Sørli et al., 2018b). Curosurf™ (a kind gift from Chiesi Farmaceutici, Italy) was used as a model LS. Leftover instillation suspensions were thawed on

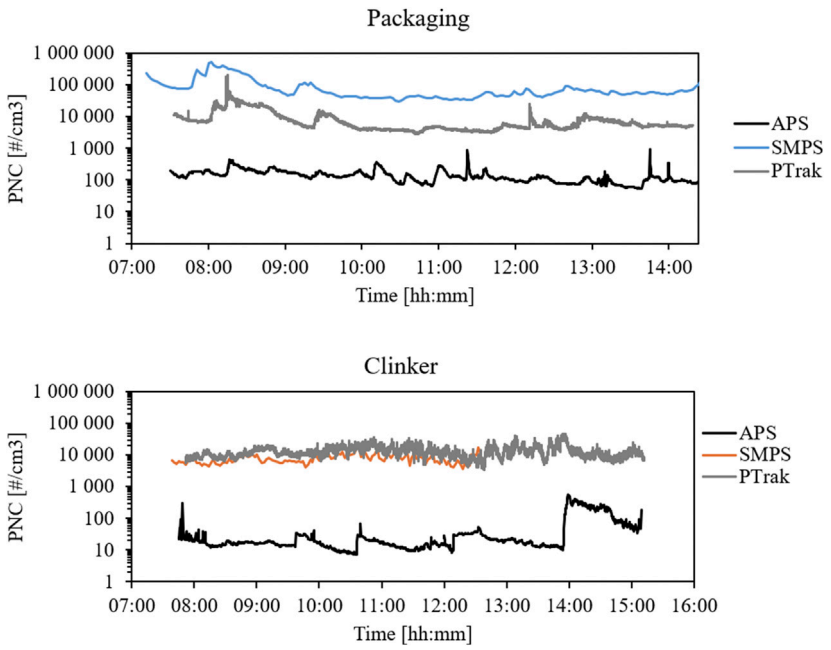


FIGURE 1
Particle number concentrations during the day shift assessed by aerodynamic particle sizer (APS), scanning mobility particle sizer (SMPS), and P-Trak at the cement bagging site (upper graph) and at the clinker production site (lower graph).

the day of testing, re-sonicated, vortexed, and mixed with LS as described below. 10 µL was placed in the CDS and recorded from the start of cycling. The final LS concentration was 2.5 mg/mL in all samples. Cycles lasted 3 s with 20%–30% compression of the maximum surface area. The 10th minimum surface tension after the start of compression was used for comparison.

LS mixed with water served as the negative control, while 0.1% Tween served as the positive control. The highest particle concentration corresponded to the highest dose used for animal exposure. Final test concentrations were: LS (water mixed with LS), Cement PM2.5 (0.216 and 0.648 µg/µg LS), Clinker PM2.5 (0.324 and 0.648 µg/µg LS), and Tween (0.02 µg/µg LS).

2.17 Statistics

Exposure data are presented as geometric means (GM). Values below the LOD were assigned half the LOD.

In vivo data were analyzed using GraphPad Prism 8.0.2 (GraphPad Software Inc., La Jolla, CA, United States). Normality and homogeneity of variance were assessed using the Shapiro-Wilk and Brown-Forsythe tests, respectively. Dose groups were compared with vehicle controls by one-way analysis of variance (ANOVA) followed by Dunnett's multiple comparison test. Gene expression data were log-transformed before analysis. $P \leq 0.05$ was considered significant.

CDS data were analyzed using RStudio (version 2025.05.1). As the data were not normally distributed, group differences were assessed using Kruskal–Wallis test. When significant, pairwise comparisons were performed using Wilcoxon rank-sum tests with Bonferroni correction. Comparison involving a single concentration were analyzed using a Wilcoxon rank-sum test.

3 Results

3.1 Personal exposure

Personal exposures to inhalable and respirable clinker and cement dust are presented in Table 1. Sampling time ranged from 412 to 463 min. GM exposures were 2.2 mg/m^3 for inhalable dust and 0.058 mg/m^3 for respirable dust. Maximum inhalable and respirable dust concentrations were 13 mg/m^3 (raw material handling and cement production) and 0.27 mg/m^3 (cement production), respectively. Inhalable dust exceeded the LOD for all workers, whereas respirable dust was below the LOD for five workers. The median respirable-to-inhalable dust ratio was 3%.

Concentrations of 14 elements in the inhalable and respirable fractions are presented in Supplementary Tables S1 and S2. Elemental concentrations were generally low, with the highest values measured for Ca and Al reaching 95 and 85 µg/m^3, respectively. Total Cr concentrations, including all oxidation stages, reached 0.27 µg/m^3. Cr(VI) was not quantified.

Mean ultrafine PNC was 13,800 particles/cm^3, although four of five workers were exposed to concentrations of 16,000–17,000 particles/cm^3 (Table 2). Mean LDSA was 40 µm^2/cm^3, mean particle size was approximately 50–60 nm, and PM0.3 was 11 µg/m^3.

3.2 Particle number concentrations

PNC for smaller particles measured by SMPS and P-Trak remained stable at the clinker production site. In contrast, larger particles measured by APS, showed an increase around 14:00, likely caused by particle resuspension when a worker passed through the area (Figure 1; Supplementary Figure S2).

TABLE 2 Personal direct-reading measurements of ultrafine particles during production and bagging.

Work task	Worker no.	Sampling time (min)	Personal breathing zone conc.							
			PNC (cm^{-3})		LDSA ($\mu m^2/cm^3$)		PM 0.3 ($\mu g/m^3$)		Particle size (nm)	
			AM ± SD	Min-max	AM ± SD	Min-max	AM ± SD	Min-max	AM ± SD	Min-max
Clinker and cement production	1	446	6,700 ± 13,000	170–412,000	19 ± 25	1.5–540	5.7 ± 11	0.1–88	59 ± 18	10–150
	4	460	16,600 ± 23,300	710–435,000	51 ± 62	5.8–1,220	15 ± 24	0.4–550	58 ± 15	16–150
	6	446	16,500 ± 53,900	280–1,660,000	43 ± 153	4.7–6,330	8.0 ± 40	0.6–1,810	61 ± 20	25–300
Cement bagging	7	424	16,100 ± 36,600	1.0–958,000	42 ± 113	0–3,090	9.0 ± 34	0.0–810	50 ± 18	12–300
	9	413	17,000 ± 40,500	160–881,000	60 ± 170	2.0–1,210	30 ± 130	0.5–920	61 ± 20	16–300

Work tasks are described in Table 1. PNC, particle number concentration; LDSA, lung-deposited surface area; AM, arithmetic mean; SD, standard deviation.

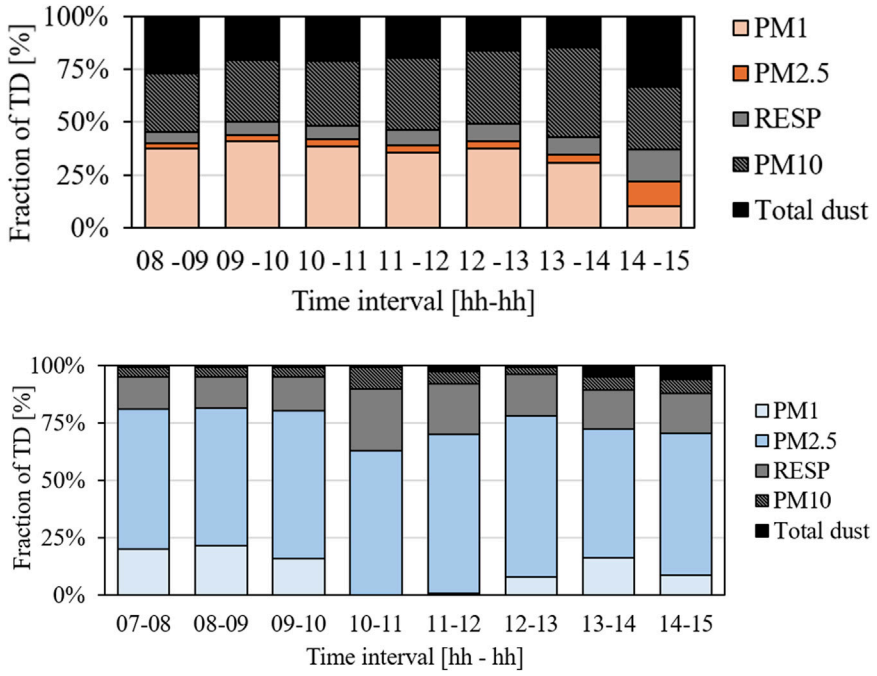


FIGURE 2
Relative contributions of PM1, PM2.5, respirable dust (RESP), and PM10 to the mass concentration of total dust at the clinker production (upper figure) and at the cement bagging site (lower figure).

PNCs in the bagging area were stable across the shift, with a gradual decline from morning levels. The initially elevated concentrations may reflect resuspension of settled dust when the rotating bagging system was started (Figure 1; Supplementary Figure S2).

At the clinker production site, mean PNCs were 47 cm^{-3} by APS (standard deviation (SD) 81), 7,860 cm^{-3} by SMPS (SD 2680), and 12,900 cm^{-3} by P-Trak (SD 5,420). Corresponding concentrations in the cement bagging area were 140 cm^{-3} (SD 70), 89,830 cm^{-3} (SD 87,180), and 8,386 cm^{-3} (SD 8,160), respectively.

3.3 Particle mass concentrations

The relative contributions of PM1, PM2.5, respirable dust, and PM10 to total dust mass concentration of total dust are shown in

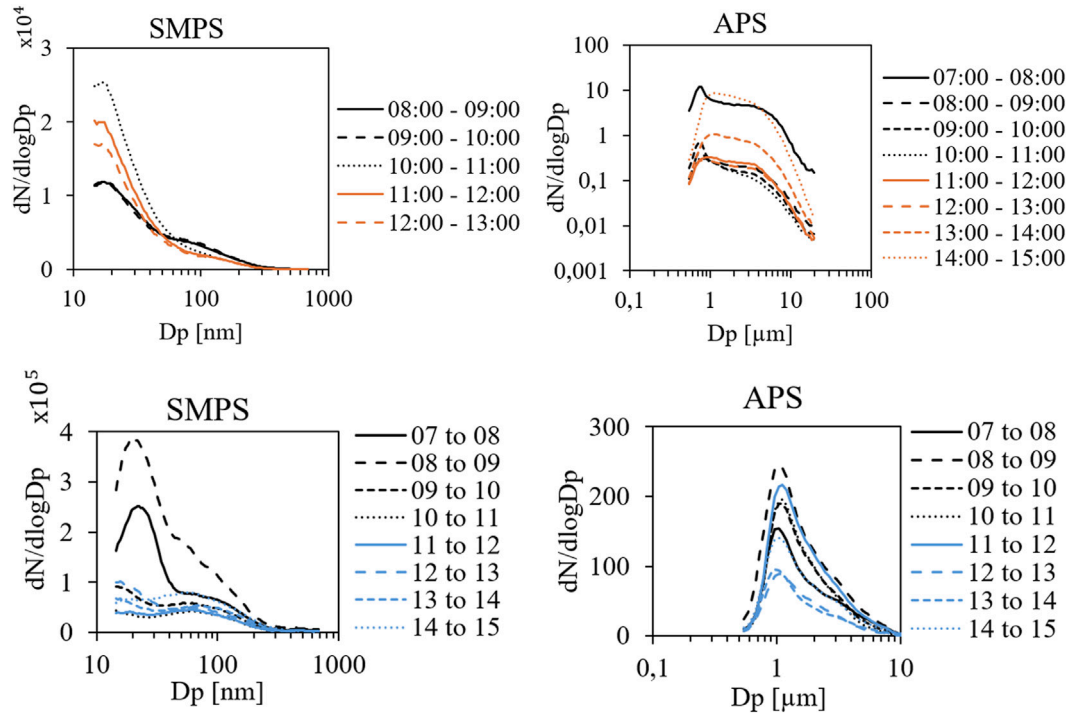


FIGURE 3
Particle number size distributions during the working shift at the clinker production (upper graph) and cement bagging site (lower graph), measured by scanning mobility particle sizer (SMPS) (14–723 nm) and aerodynamic particle sizer (APS) (0.5–20 µm).

Figure 2. The increase in PNC around 14:00 at the clinker production site was also reflected in the mass measurements, where the relative contribution of PM1 and PM2.5 decreased. This supports the interpretation that the peak was caused by resuspended coarse particles. The respirable fraction accounted for approximately 75% of total dust at the clinker production and generally exceed 90% in the cement bagging area.

3.4 Particle size distributions

Particle number size distributions were bimodal at both the clinker production and cement bagging sites (Figure 3). The increased micrometer-mode concentration during the first and last hours at the clinker production site likely reflected activities associated with starting and ending the measurement campaign. At both sites, most particles by number were 20–30 nm.

3.5 Chemical composition of PM2.5

Clinker PM2.5 and Cement PM2.5 consisted primarily of Ca, accounting for 55% and 62%, respectively. Other major constituents were Al (21% and 15%), Fe (15% in both), and Mg (8% and 7%). Clinker PM2.5, but not Cement PM2.5, contained 0.6% Zn. Trace amounts of additional metals were detected in the respirable and inhalable fractions. All constituents above the LOD are listed in Supplementary Table S3. Synchrotron-based X-ray absorption spectroscopy showed differences in Fe speciation between Clinker PM2.5 and Cement PM2.5. Fe in clinker consisted of 44% ferrihydrite, 40% nontronite, and 14% jarosite, whereas Fe in cement consisted of 67% ferrihydrite, 18% jarosite, and 16% nontronite.

3.6 Microbial contamination

Cement PM2.5 contained low but detectable endotoxin levels by LAL assay (1.8 EU/mg), whereas endotoxin in Clinker PM2.5 was below the LOD. Neither material activated the HEK-Blue™ hTLR2 or hTLR4 reporter cell lines. Relative SEAP responses remained near baseline for both materials and receptors: TLR2, 1.07 ± 0.05 for Cement PM2.5 and 1.01 ± 0.07 for Clinker PM2.5; TLR4, 1.05 ± 0.07 for Cement PM2.5 and 1.08 ± 0.18 for Clinker PM2.5 (Supplementary Figure S3).

3.7 *In vivo* instillation suspensions

Both suspensions showed bimodal size distributions that varied with concentration (Supplementary Figure S4). The intensity-based z-average hydrodynamic size decreased with particle concentration, indicating concentration-dependent agglomeration. Clinker PM2.5 consistently had larger z-average sizes than Cement PM2.5. Polydispersity index values ranged from 0.28 to 0.55, indicated moderately polydisperse suspensions, with greater heterogeneity at lower concentrations (Supplementary Table S4).

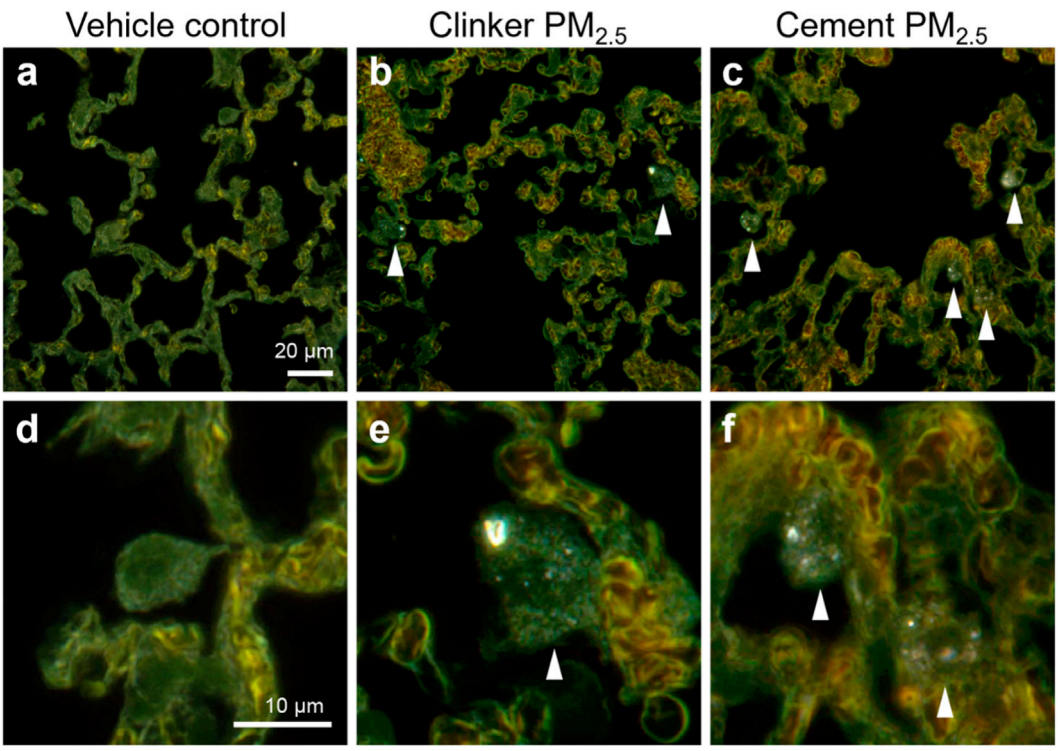


FIGURE 4
Mouse lung tissue 28 days after intratracheal exposure to **(a,d)** vehicle control, **(b,e)** 162 µg/mouse clinker PM2.5 or **(c,f)** 162 µg/mouse cement PM2.5. Particles appear as bright dots and aggregates in alveolar macrophages (arrowheads). Enhanced darkfield microscopy of eosin-stained lung.

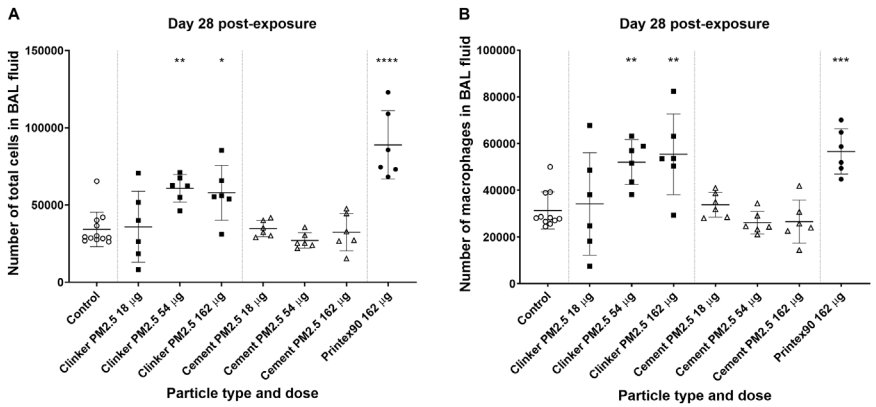


FIGURE 5
Total cell **(A)** and macrophage **(B)** counts in bronchoalveolar lavage (BAL) fluid 28 days post-exposure. Data are presented as individual values with mean ± standard deviation (SD). n = 6 mice per dose; N = 12 vehicle control mice. Asterisks indicate statistically significant differences compared with the vehicle control group (Dunnett's multiple comparisons test). Significance levels: *P ≤ 0.05; **P ≤ 0.01; ***P ≤ 0.001; ****P ≤ 0.0001.

3.8 Biopersistence in mouse lung tissue

28 days post-exposure, low levels of particles were detected in alveolar macrophages from mice exposed to both Clinker PM2.5 or Cement PM2.5 (Figure 4). Most particles were nanoscale, although the resolution limit was approximately 200 nm, and a few micrometer-sized aggregates were observed.

3.9 Cytotoxicity and total protein

Viability remained high across groups. A small reduction in mean viability was observed at day 28 in mice after exposure to the highest Clinker PM2.5 dose (Supplementary Figure S5). BAL LDH activity at the highest dose did not differ significantly from controls for either material at any time

10.3389/ftox.2026.1963820

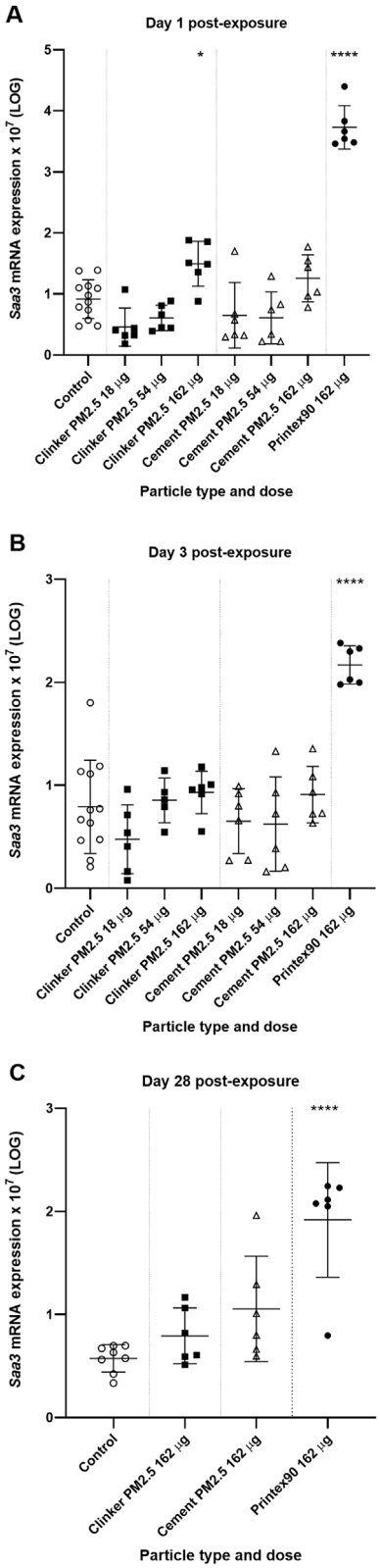


FIGURE 6
Pulmonary *Saa3* mRNA expression levels 1 day **(A)**, 3 days **(B)**, and 28 days **(C)** post-exposure. Data are log transformed and presented as individual values with mean ± standard deviation (SD). n = 6 mice per dose; N = 12 vehicle control mice. Asterisks indicate statistically significant differences compared with the vehicle control group (Dunnett's multiple comparisons test). Significance levels: *P ≤ 0.05; ****P ≤ 0.01.

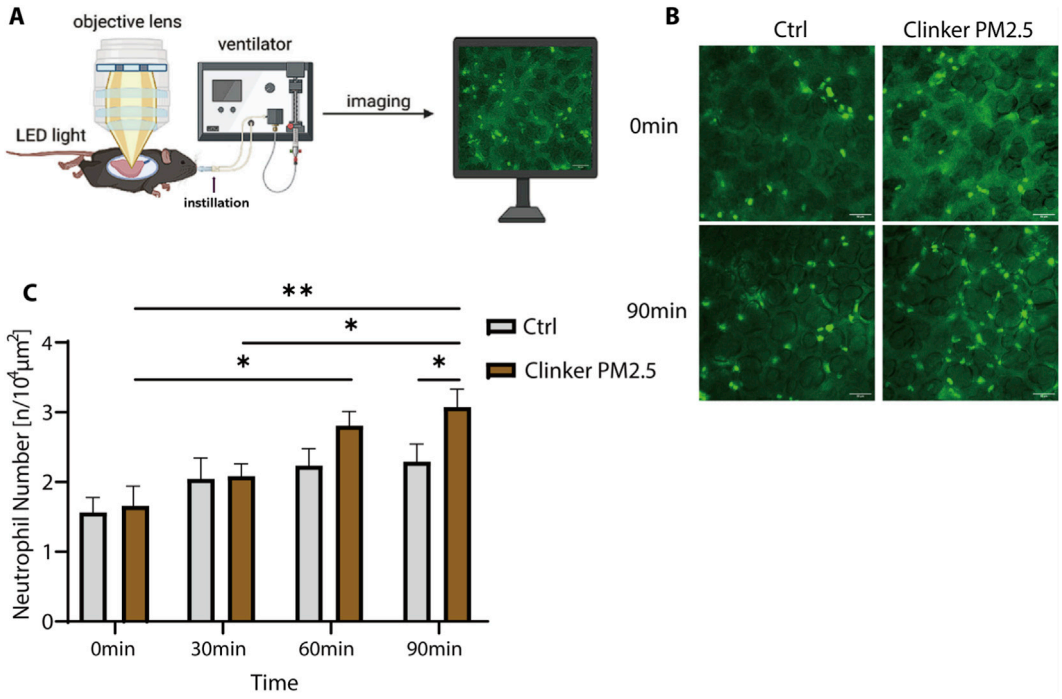


FIGURE 7
(A) Schematic overview of lung intravital microscopy (L-IVM) following intratracheal instillation of Clinker PM2.5 in mice. **(B)** Representative L-IVM images showing neutrophils (anti-Ly6G mAbs, intravenous, green) in the alveolar region at 0 min and 90 min after intratracheal instillation of vehicle (50 µL 2% mouse serum) or Clinker PM2.5 (162 µg/50 µL per mouse). Scale bar, 50 µm. **(C)** Quantification of neutrophil numbers over time. Data are presented as mean ± standard error of the mean (SEM), n = 3 mice per group. *: $P < 0.05$ and **: $P < 0.01$ using two-way ANOVA.

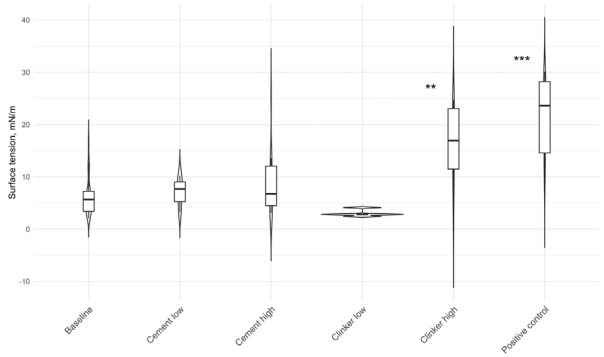


FIGURE 8
Median minimum surface tension at the 10th compression cycle for each test condition. Baseline: lung surfactant (LS, 2.5 mg/mL water), i.e., the final LS concentration in all test conditions. Cement PM2.5 low and high contain 0.216 and 0.648 µg/µg LS respectively. Clinker PM2.5 low and high contains 0.324 and 0.648 µg/µg LS respectively. Positive control (0.02 µg Tween/µg LS). Baseline and positive control data were pooled across experimental days; all other conditions were tested on a single day. ** $P < 0.01$, *** $P < 0.001$ vs. baseline.

point (Supplementary Figure S6). Likewise, BAL protein concentrations showed no consistent or dose-dependent increases following Clinker PM2.5 or Cement PM2.5 exposure (Supplementary Figure S7). In contrast, Printex90 increased BAL protein at all time points, consistent with previous findings (Danielsen et al., 2020; Di Battista et al., 2024; Hadrup et al., 2021; Hadrup et al. 2019; Hadrup et al. 2020a; Saber et al., 2012b).

3.10 Inflammatory cell response

Clinker PM2.5 caused modest increases in total BAL cell numbers, particularly at day 28, when significant increases were observed at 54 µg and 162 µg (Figure 5A). Cement PM2.5 did not affect total BAL cell numbers at any time point (Supplementary Table S5). Macrophages increased at day 28 after Clinker PM2.5 exposure but not after Cement PM2.5 exposure (Figure 5B). Neutrophil, lymphocytes, and eosinophil numbers remained low for both materials. A significant increase in lymphocytes was observed at day 28 after exposure to 54 µg Clinker PM2.5 (Supplementary Table S5).

3.11 Acute phase response in lung and liver

At day 1, Clinker PM2.5 significantly increased pulmonary *Saa3* expression compared with vehicle controls, whereas Cement PM2.5 had no effect (Figure 6A). At later time points, *Saa3* expression was comparable to controls for both materials. No significant differences in hepatic acute phase response, in terms of *Saa1*, were observed between exposed and control groups (Supplementary Figure S8).

3.12 Neutrophil recruitment in alveolar microvessels

Neutrophil numbers increased 60 min after Clinker PM2.5 instillation. At 90 min, neutrophil numbers were significantly higher than controls (Figure 7B,C).

3.13 Inhibition of lung surfactant (LS) function

Clinker PM2.5 increased surface tension at 0.648 μg/μg LS, and the increase was significant above baseline. In contrast, Cement PM2.5 did not affect surfactant function (Figure 8).

4 Discussion

Occupational exposure to airborne particles was assessed across key stages of cement production including clinker production and bagging, using filter-based sampling and portable direct-reading instruments. GM personal exposure was 2.2 mg/m^3 for inhalable dust and 0.058 mg/m^3 for respirable dust. These levels were lower than those reported in European cement workers, where average inhalable and respirable dust concentrations ranged from 2.8 to 0.24 mg/m^3 and 3.6 and 0.32 mg/m^3, respectively (Fell et al., 2011; Notø et al., 2016). In contrast, inhalable dust exposure during bagging (1.6–3.6 mg/m^3) was comparable to measurements from Italian cement workers (1.6–3.8 mg/m^3) (Fontanella et al., 2026). Previous studies identified work tasks such as bagging, shipping, raw meal handling, and cleaning as major contributors to dust exposure in cement production (Notø et al., 2017).

For inhalable non-specific inorganic dust, occupational exposure limits (OELs) are typically in the range of 5–10 mg/m^3, while respirable dust limits range from 2.5 to 5 mg/m^3 (Danish Working Environment Authority, 2025; Swedish Work Environment Authority, 2023). Although average exposures were below current OELs, one worker exceeded the Swedish and Danish inhalable dust OELs, while another had exposure close to the Swedish limit (5 mg/m^3), but below the Danish OEL (10 mg/m^3). Because occupational dust exposure varies considerably between workdays, maintaining exposure below OELs is desirable. This is particularly relevant because reduced lung function has been reported at inhalable dust concentrations of 9.2 mg/m^3 (Nordby et al., 2016), and declines in lung function have also been observed at total dust concentrations ≥4.5 mg/m^3 and respirable dust concentrations ≥2.3 mg/m^3 (Fell and Nordby, 2017).

Thus, exposure levels approaching current OELs may still be of concern for respiratory health. These findings should also be considered within the broader hierarchy of occupational controls, which prioritizes elimination or substitution and engineering controls over administrative measures and personal protective equipment (Ajslev et al., 2022). Engineering controls may be particularly relevant for dust-generating operations such as bagging. Although investigated in industrial mineral rather than cement production, Louk et al. (2020) showed that engineering and process controls, including local exhaust ventilation and modifications to bagging systems, can reduce respirable dust exposure during bagging. Similar source-oriented approaches may therefore also be relevant for reducing dust exposure in cement production.

More broadly, inorganic mineral dusts differ in their health effects depending on composition and fibrogenic potential, and chronic exposure to fibrogenic dusts can cause irreversible occupational lung diseases. This further supports proactive source-oriented dust control, including source containment, local exhaust ventilation, and other engineering measures, rather than relying primarily on personal respiratory protection. Even when average dust concentrations are below current OELs, maintaining exposures as low as reasonably achievable is therefore an important preventive strategy.

The respirable-to-inhalable dust ratio was 3%, considerably lower than the 9% previously reported for European and Norwegian cement workers (Fell et al., 2011; Notø et al., 2016), suggesting fewer fine and ultrafine particles in the investigated plant. Cement dust typically spans particle sizes from the submicrometer range to approximately 100 μm (Ferraris et al., 2004), while 85 wt% of raw meal particles are smaller than 90 μm (Notø, 2019). Although a trend toward finer cement grinding has been proposed (Notø, 2019), potentially increasing respirable dust exposure, this was not reflected in the present measurements.

Personal exposure characterized by LDSA, PNC, and PM0.3 has rarely been reported for cement production workers. The cement workers were exposed to LDSA levels of 40 μm^2 cm^{-3} which is similar to that reported for post-fire workers (36 μm^2 cm^{-3}), but lower than levels measured among asphalt millers (67 μm^2 cm^{-3}), pavers (80 μm^2 cm^{-3}), personnel around fires (65 μm^2 cm^{-3}), firefighters (680 μm^2 cm^{-3}) (Hedmer et al., 2026; Loven et al., 2024) as well as chimney sweepers (Moazami et al., 2024), and workers handling engineered nanomaterials (Loven et al., 2021).

Likewise, average PNCs in the PBZ (~16,000–17,000 particles/cm^3) for the cement workers were considerably lower than those reported for asphalt workers (31,000 particles/cm^3), tunnel workers (48,000 particles/cm^3, and firefighters (65,000 particles/cm^3) (Hedmer et al., 2026; Hedmer et al., 2017; Loven et al., 2024). Our findings are consistent with previous stationary measurements in cement production where the concentration similarly was low (20,000 particles/cm^3) (Ervik et al., 2022). Particles emitted during cement production mainly origin from mechanical processes generating coarse particles, whereas ultrafine particles primarily arise from high-temperature kiln processes and consist mainly from soot and secondary volatile particles (Ervik et al., 2022). Because of the kiln's proximity, there is a high degree of interference from the heating process, where particles <100 nm are likely to be present also in the cooling corridor as well. This, however, is a part of the process and hence part of the exposure, especially for workers in the clinker production area.

This exploratory study included few workers, with personal exposure measured on a single workday per participant. Stationary measurements represented selected production areas and may not fully reflect individual exposure because workers moved between tasks during the shift. Consequently, stationary measurements at specific locations provide only a limited snapshot of workers' exposure, which may explain why the different particle fractions were not always comparable between personal and stationary measurements. The plant was sampled close to the annual shutdown for cleaning, indicating that the plant likely was

in one of the dustiest states of the year, which could have contributed to dust accumulation and resuspension. Future studies would benefit from repeated measurements across additional production stages, including cleaning and maintenance activities and control rooms, where workers may spend much of their shift.

Although, inhalation is the gold standard for risk assessment, intratracheal instillation is suitable for hazard assessment, particularly when limited amounts of field-collected material are available (Saber et al., 2012a). This approach has previously been used to assess toxicity of different particulates including sanding dusts (Saber et al., 2012a; Saber et al. 2012b; Saber et al. 2016), diesel and jet-engine emissions (Bendtsen et al., 2019; Bendtsen et al., 2020) and occupationally relevant particles (Gutierrez et al., 2023).

Both materials induced mild pulmonary effects. Clinker PM2.5 produced stronger responses than Cement PM2.5, including modest increases in BAL cell counts and an early pulmonary acute phase response, a response that has been linked to risk of cardiovascular disease (Hadrup et al., 2020b; Saber et al., 2014). L-IVM demonstrated rapid neutrophil recruitment within 1 h of Clinker PM2.5 exposure, indicating an early innate immune response. Both materials persisted in alveolar macrophages 28 days after exposure. These finding indicate small differences in toxicity, despite the similar industrial origin and elemental composition of the materials.

Trace amounts of Zn were detected in Clinker PM2.5 but not in Cement PM2.5 and may have contributed to the stronger response. Further analyses, for example, by X-ray absorption spectroscopy (XAS), would be required to determine the chemical form of Zn. XAS analysis of Fe also indicated differences in iron oxide composition, with a slightly higher Fe oxidation state in Clinker PM2.5 than in Cement PM2.5. This difference may have contributed to the greater response of Clinker PM2.5.

LS forms a protective layer at the alveolar air–liquid interface and reduces surface tension during expiration, preventing alveolar collapse and supporting normal breathing (Sørli et al., 2018b) as indicated in adverse outcome pathway 302 linking inhibition of LS function to reduced lung function (Da Silva et al., 2021). Assuming a total LS mass of 0.15 mg in mice (Sørli et al., 2018a), the highest administered particle dose corresponded to approximately 1.1 μg particle per μg LS. The highest concentrations tested in the CDS was 0.648 μg particle per μg LS. At this concentration, Clinker PM2.5, but not Cement PM2.5 inhibited LS function. However, this was not accompanied by increased BAL LDH activity 1 day after exposure, suggesting no measurable acute loss of membrane integrity under the tested conditions exposure.

5 Conclusion

Overall, workers were exposed to relatively low average concentrations of respirable dust, and ultrafine particle exposure was also low compared with several other occupations. The collected PM2.5 samples induced mild pulmonary responses *in vivo*, with slight differences between samples from the clinker production and cement bagging sites.

Data availability statement

The original contributions presented in the study are included in the article/Supplementary Material, further inquiries can be directed to the corresponding author.

Ethics statement

Ethical approval was not required for the studies on humans in accordance with the local legislation and institutional requirements because only commercially available established cell lines were used. The animal study was approved by Danish Animal Experiments Inspectorate at the Danish Ministry of Justice (license 2020-15-0201-00485) and Regierung von Oberbayern (District Government of Upper Bavaria) under the approval number ROB-55.2Vet-2532.Vet_02-19-150. The study was conducted in accordance with the local legislation and institutional requirements.

Author contributions

PD: Data curation, Visualization, Investigation, Writing – original draft, Writing – review and editing, Conceptualization, Formal Analysis, Methodology. MH: Writing – review and editing, Conceptualization, Investigation, Formal Analysis, Methodology, Writing – original draft, Visualization, Data curation. CA: Writing – original draft, Formal Analysis, Visualization, Data curation, Writing – review and editing, Methodology, Investigation. TB: Writing – review and editing, Formal Analysis, Methodology, Writing – original draft, Data curation, Investigation, Visualization. MS: Methodology, Writing – original draft, Data curation, Visualization, Investigation, Writing – review and editing. JS: Visualization, Data curation, Formal Analysis, Methodology, Writing – review and editing, Investigation, Writing – original draft. MK: Visualization, Investigation, Writing – original draft, Writing – review and editing, Methodology, Formal Analysis, Data curation. PL: Writing – review and editing, Writing – original draft, Methodology, Formal Analysis, Investigation, Visualization, Data curation. JE: Methodology, Data curation, Visualization, Writing – original draft, Investigation, Writing – review and editing. GY: Formal Analysis, Data curation, Writing – original draft, Visualization, Writing – review and editing, Investigation, Methodology. MR: Writing – review and editing, Investigation, Writing – original draft, Data curation, Visualization, Methodology. CI: Investigation, Writing – review and editing, Conceptualization, Funding acquisition, Writing – original draft, Data curation, Formal Analysis, Visualization, Project administration, Methodology. UV: Conceptualization, Investigation, Writing – review and editing, Funding acquisition, Project administration, Data curation, Writing – original draft, Visualization, Methodology, Formal Analysis.

Funding

The author(s) declared that financial support was received for this work and/or its publication. This work was supported by the European Union under the HORIZON-CL4-2022-DIGITAL-EMERGING-01 program (NanoPASS – GA101092741) and by

AFA Insurance (160226). We acknowledge the MAX IV Laboratory for beamtime on the Balder beamline under proposal 20220629. Research conducted at MAX IV, a Swedish national user facility, is supported by Vetenskapsrådet (Swedish Research Council, VR) under contract 2018-07152, Vinnova (Swedish Governmental Agency for Innovation Systems) under contract 2018-04969 and Formas under contract 2019-02496.

Acknowledgments

The excellent technical assistance from Michael Guldbrandsen, Eva Terrida, and Hatice Gülen from the National Research Centre for the Working Environment is greatly appreciated. The authors express their gratitude toward the cement producer and cement production workers for their participation in the study. We extend our gratitude to Associate Professor Jenny Rissler at Ergonomics and Aerosol Technology for the detailed assessment of chemical form of cement and clinker at MAX IV Synchrotron radiation facility at Lund University, and the subsequent spectral analyses.

Conflict of interest

The author(s) declared that this work was conducted in the absence of any commercial or financial relationships that could be construed as a potential conflict of interest.

Generative AI statement

The author(s) declared that generative AI was not used in the creation of this manuscript.

Any alternative text (alt text) provided alongside figures in this article has been generated by Frontiers with the support of artificial intelligence and reasonable efforts have been made to ensure accuracy, including review by the authors wherever possible. If you identify any issues, please contact us.

Publisher's note

All claims expressed in this article are solely those of the authors and do not necessarily represent those of their affiliated organizations, or those of the publisher, the editors and the reviewers. Any product that may be evaluated in this article, or claim that may be made by its manufacturer, is not guaranteed or endorsed by the publisher.

Supplementary material

The Supplementary Material for this article can be found online at: https://www.frontiersin.org/articles/10.3389/ftox.2026.1963820/full#supplementary-material

References

Ajslev, J. Z. N., Møller, J. L., Andersen, M. F., Pirzadeh, P., and Lingard, H. (2022). The hierarchy of controls as an approach to visualize the impact of occupational safety and health coordination. *Int. J. Environ. Res. Public Health*, 19, 2731 doi: 10.3390/ijerph19052731

Aranda-Usón, A., López-Sabirón, A. M., Ferreira, G., and Llera Sastresa, E. (2013). Uses of alternative fuels and raw materials in the cement industry as sustainable waste management options. *Renew. Sustain. Energy Rev.* 23, 242–260. doi: 10.1016/j.rser.2013.02.024

Bendtsen, K. M., Brostrom, A., Koivisto, A. J., Koponen, I., Berthing, T., Bertram, N., et al. (2019). Airport emission particles: exposure characterization and toxicity following intratracheal instillation in mice. *Part Fibre Toxicol.* 16 (1), 23. doi: 10.1186/s12989-019-0305-5

Bendtsen, K. M., Gren, L., Malmborg, V. B., Shukla, P. C., Tunér, M., Essig, Y. J., et al. (2020). Particle characterization and toxicity in C57BL/6 mice following instillation of five different diesel exhaust particles designed to differ in physicochemical properties. *Part Fibre Toxicol.* 17 (1), 38. doi: 10.1186/s12989-020-00369-9

Berthing, T., Lard, M., Danielsen, P. H., Abariute, L., Barfod, K. K., Adolfsson, K., et al. (2023). Pulmonary toxicity and translocation of gallium phosphide nanowires to secondary organs following pulmonary exposure in mice. *J. Nanobiotechnol* 21 (1), 322. doi: 10.1186/s12951-023-02049-0

Danielsen, P. H., Knudsen, K. B., Strancar, J., Umek, P., Koklič, T., Garvas, M., et al. (2020). Effects of physicochemical properties of TiO(2) nanomaterials for pulmonary inflammation, acute phase response and alveolar proteinosis in intratracheally exposed mice. *Toxicol. Appl. Pharmacol.* 386, 114830. doi: 10.1016/j.taap.2019.114830

Danielsen, P. H., Bendtsen, K. M., Knudsen, K. B., Poulsen, S. S., Stoeger, T., and Vogel, U. (2021). Nanomaterial- and shape-dependency of TLR2 and TLR4 mediated signaling following pulmonary exposure to carbonaceous nanomaterials in mice. *Part Fibre Toxicol.* 18 (1), 40. doi: 10.1186/s12989-021-00432-z

Danielsen, P. H., Poulsen, S. S., Mortensen, A., Berthing, T., Gargouri, D., Filoramo, A., et al. (2025). Imogolite nanotube modifications impact pulmonary toxicity in mice: implications for safe and sustainable by design (SSbD). *J. Nanobiotechnol* 23 (1), 571. doi: 10.1186/s12951-025-03647-w

Danish Working Environment Authority (2025). Bekendtgørelse om grænseværdier for stoffer og materialer (kemiske agenser) i arbejdsmiljøet jf.

Da Silva, E., Vogel, U., Hougaard, K. S., Perez-Gil, J., Zuo, Y. Y., and Sorli, J. B. (2021). An adverse outcome pathway for lung surfactant function inhibition leading to decreased lung function. *Curr. Res. Toxicol.* 2, 225–236. doi: 10.1016/j.crtox.2021.05.005

Di Battista, V., Danielsen, P. H., Gajewicz-Skretna, A., Kedziorski, A., Seiffert, S. B., Ma-Hock, L., et al. (2024). Oxide-perovskites for automotive catalysts biotransform and induce multicomponent clearance and hazard. *ACS Nano* 18 (47), 32672–32693. doi: 10.1021/acsnano.4c10135

Ervik, T. K., Eriksen Hammer, S., Noto, H., Ellingsen, D. G., Thomassen, Y., Weinbruch, S., et al. (2022). Physicochemical characterization of particulate matter in a cement production plant. *Environ. Sci. Process Impacts* 24 (8), 1243–1256. doi: 10.1039/d2em00139j

Fell, A. K. M., and Nordby, K. C. (2017). Association between exposure in the cement production industry and non-malignant respiratory effects: a systematic review. *BMJ Open* 7 (4), e012381. doi: 10.1136/bmjopen-2016-012381

Fell, A. K., Sikkeland, L. I., Svendsen, M. V., and Kongerud, J. (2010). Airway inflammation in cement production workers. *Occup. Environ. Med.* 67 (6), 395–400. doi: 10.1136/oem.2009.047852

Fell, A. K., Noto, H., Skogstad, M., Nordby, K. C., Eduard, W., Svendsen, M. V., et al. (2011). A cross-shift study of lung function, exhaled nitric oxide and inflammatory markers in blood in Norwegian cement production workers. *Occup. Environ. Med.* 68 (11), 799–805. doi: 10.1136/oem.2010.057729

Ferraris, C. F., Hackley, V. A., and Avilés, A. I. (2004). Measurement of particle size distribution in Portland cement powder: analysis of ASTM round robin studies. *Cem. Concr. Aggr* 26 (2), 71–81. doi: 10.1520/cca11920

Fontanella, M. C., Serena, E., Guarascio, D., and Beone, G. M. (2026). Occupational exposure to antimony from cement additives: speciation and health risk insights. *Chemosphere* 399, 144894. doi: 10.1016/j.chemosphere.2026.144894

Gutierrez, C. T., Loizides, C., Hafez, I., Brostrøm, A., Wolff, H., Szarek, Z., et al. (2023). Acute phase response following pulmonary exposure to soluble and insoluble metal oxide nanomaterials in mice. *Part Fibre Toxicol.* 20 (1), 4. doi: 10.1186/s12989-023-00514-0

Hadrup, N., Bengtson, S., Jacobsen, N. R., Jackson, P., Nocun, M., Saber, A. T., et al. (2017). Influence of dispersion medium on nanomaterial-induced pulmonary inflammation and DNA strand breaks: investigation of carbon black, carbon nanotubes and three titanium dioxide nanoparticles. *Mutagenesis* 32 (6), 581–597. doi: 10.1093/mutage/gex042

Hadrup, N., Knudsen, K. B., Berthing, T., Wolff, H., Bengtson, S., Kofoed, C., et al. (2019). Pulmonary effects of nanofibrillated celluloses in mice suggest that carboxylation lowers the inflammatory and acute phase responses. *Environ. Toxicol. Pharmacol.* 66, 116–125. doi: 10.1016/j.etap.2019.01.003

Hadrup, N., Saber, A. T., Kyjovska, Z. O., Jacobsen, N. R., Vippola, M., Sarlin, E., et al. (2020a). Pulmonary toxicity of Fe(2)O(3), ZnFe(2)O(4), NiFe(2)O(4) and NiZnFe(4)O(8) nanomaterials: inflammation and DNA strand breaks. *Environ. Toxicol. Pharmacol.* 74, 103303. doi: 10.1016/j.etap.2019.103303

Hadrup, N., Zhernovkov, V., Jacobsen, N. R., Voss, C., Strunz, M., Ansari, M., et al. (2020b). Acute phase response as a biological mechanism-of-action of (Nano)particle-Induced cardiovascular disease. *Small* 16 (21), e1907476. doi: 10.1002/smll.201907476

Hadrup, N., Aimonen, K., Ilves, M., Lindberg, H., Atluri, R., Sahlgren, N. M., et al. (2021). Pulmonary toxicity of synthetic amorphous silica - effects of porosity and copper oxide doping. *Nanotoxicol* 15 (1), 96–113. doi: 10.1080/17435390.2020.1842932

Hadrup, N., Guldbrandsen, M., Terrida, E., Bendtsen, K. M. S., Hougaard, K. S., Jacobsen, N. R., et al. (2025). Intratracheal instillation for the testing of pulmonary toxicity in mice-Effects of instillation devices and feed type on inflammation. *Anim. Model Exp. Med.* 8 (2), 378–386. doi: 10.1002/ame2.12503

Hedmer, M., Wierzbicka, A., Li, H. Q., Albin, M., Tinnerberg, H., and Broberg, K. (2017). Diesel exhaust exposure assessment among tunnel construction workers-correlations between nitrogen dioxide, respirable elemental carbon, and particle number. *Ann. Work Expos Heal* 61 (5), 539–553. doi: 10.1093/annweh/wxx024

Hedmer, M., Loven, K., Rex, J., Nilsson, C. A., Polat, M., Nøjgaard, J. K., et al. (2026). Characterization of occupational exposure to air pollutants during asphalt milling and paving. *Ann. Work Expo. Health* 70 (2), wxaf078. doi: 10.1093/annweh/wxaf078

Isaxon, C., Loven, K., Ludvigsson, L., Sivakumar, S., Gudmundsson, A., Messing, M. E., et al. (2020). Workplace emissions and exposures during semiconductor nanowire production, post-production, and maintenance work. *Ann. Work Expo. Health* 64 (1), 38–54. doi: 10.1093/annweh/wxz088

Jackson, P., Lund, S. P., Kristiansen, G., Andersen, O., Vogel, U., Wallin, H., et al. (2011). An experimental protocol for maternal pulmonary exposure in developmental toxicology. *Basic Clin. Pharmacol. Toxicol.* 108 (3), 202–207. doi: 10.1111/j.1742-7843.2010.00644.x

Lei, P., Zegeye, F. D., Alswady-Hoff, M., Marcolungo, C., Danielsen, P. H., Madsen, A. M., et al. (2025). Detection of microbial contamination in nanomaterials using LAL, rFC and cell-based assays: implications for nanotoxicological hazard assessment. *Nanomater. (Basel)* 15 (24), 1871. doi: 10.3390/nano15241871

Li, C., Liu, Q., Han, L., Zhang, H., Immler, R., Rathkolb, B., et al. (2024). The eATP/P2x7R axis drives quantum dot-nanoparticle induced neutrophil recruitment in the pulmonary microcirculation. *Adv. Sci. (Weinh)* 11 (45), e2404661. doi: 10.1002/advs.202404661

Liu, Q., Yang, L., Li, C., Han, L., Wilmot, J., Yang, G., et al. (2025). Alveolar macrophages initiate the spatially targeted recruitment of neutrophils after nanoparticle inhalation. *Sci. Adv.* 11, eadx8586. doi: 10.1126/sciadv.adx8586

Louk, A. K., Patts, J. R., Haas, E. J., and Cecala, A. B. (2020). Evaluation of engineering controls at bagging operations to reduce exposures to respirable crystalline silica dust. *Min. Metall. Explor* 37 (4), 1055–1064. doi: 10.1007/s42461-020-00210-z

Loven, K., Franzen, S. M., Isaxon, C., Messing, M. E., Martinsson, J., Gudmundsson, A., et al. (2021). Emissions and exposures of graphene nanomaterials, titanium dioxide nanofibers, and nanoparticles during down-stream industrial handling. *J. Expo. Sci. Environ. Epidemiol.* 31 (4), 736–752. doi: 10.1038/s41370-020-0241-3

Loven, K., Hagvall, L., Rex, J., Nilsson, C. A., Malmborg, V., Pagels, J., et al. (2024). Characterization of exposure to air pollutants for workers in and around fires. *J. Occup. Environ. Hyg.* 21 (12), 878–894. doi: 10.1080/15459624.2024.2406244

Moazami, T. N., Jørgensen, R. B., Svendsen, K. V. H., Teigen, K. A., and Hegseth, M. N. (2024). Personal exposure to gaseous and particulate phase polycyclic aromatic hydrocarbons (PAHs) and nanoparticles and lung deposited surface area (LDSA) for soot among Norwegian chimney sweepers. *J. Occup. Environ. Hyg.* 21 (1), 24–34. doi: 10.1080/15459624.2023.2264349

Nordby, K. C., Noto, H., Eduard, W., Skogstad, M., Fell, A. K., Thomassen, Y., et al. (2016). Thoracic dust exposure is associated with lung function decline in cement production workers. *Eur. Respir. J.* 48 (2), 331–339. doi: 10.1183/13993003.02061-2015

Notø, H. P. (2019). "Dust exposure among European cement production workers," in *Determinants of Thoracic Aerosol Exposure and Relationships between different Aerosol Fractions [doctoral dissertation]*. Oslo, Norway: University of Oslo.

Notø, H. P., Nordby, K. C., and Eduard, W. (2016). Relationships between personal measurements of 'total' dust, respirable, thoracic, and inhalable aerosol fractions in the cement production industry. *Ann. Occup. Hyg.* 60 (4), 453–466. doi: 10.1093/annhyg/mev093

Notø, H., Nordby, K. C., Skare, O., and Eduard, W. (2017). Job tasks as determinants of thoracic aerosol exposure in the cement production industry. *Ann. Work Expo. Health* 62 (1), 88–100. doi: 10.1093/annweh/wxx085

Poulsen, S. S., Knudsen, K. B., Jackson, P., Weydahl, I. E. K., Saber, A. T., Wallin, H., et al. (2017). Multi-walled carbon nanotube-physicochemical properties predict the systemic acute phase response following pulmonary exposure in mice. *PLoS One* 12 (4), e0174167. doi: 10.1371/journal.pone.0174167

Saber, A. T., Halappanavar, S., Folkmann, J. K., Bornholdt, J., Boisen, A. M. Z., Møller, P., et al. (2009). Lack of acute phase response in the livers of mice exposed to diesel exhaust particles or carbon black by inhalation. *Part Fibre Toxicol.* 6, 12. doi: 10.1186/1743-8977-6-12

Saber, A. T., Mortensen, A., Szarek, J., Koponen, I. K., Levin, M., Jacobsen, N. R., et al. (2016). Epoxy composite dusts with and without carbon nanotubes cause similar pulmonary responses, but differences in liver histology in mice following pulmonary deposition. *Part Fibre Toxicol.* 13 (1), 37. doi: 10.1186/s12989-016-0148-2

Saber, A. T., Jacobsen, N. R., Mortensen, A., Szarek, J., Jackson, P., Madsen, A. M., et al. (2012a). Nanotitanium dioxide toxicity in mouse lung is reduced in sanding dust from paint. *Part Fibre Toxicol.* 9, 4. doi: 10.1186/1743-8977-9-4

Saber, A. T., Jensen, K. A., Jacobsen, N. R., Birkedal, R., Mikkelsen, L., Møller, P., et al. (2012b). Inflammatory and genotoxic effects of nanoparticles designed for inclusion in paints and lacquers. *Nanotoxicol* 6 (5), 453–471. doi: 10.3109/17435390.2011.587900

Saber, A. T., Jacobsen, N. R., Jackson, P., Poulsen, S. S., Kyjovska, Z. O., Halappanavar, S., et al. (2014). Particle-induced pulmonary acute phase response may be the causal link between particle inhalation and cardiovascular disease. *Wiley Interdiscip. Rev. Nanomed Nanobiotechnol* 6 (6), 517–531. doi: 10.1002/wnan.1279

Sørli, J. B., Balogh Sivars, K., Da Silva, E., Hougaard, K. S., Koponen, I. K., Zuo, Y. Y., et al. (2018a). Bile salt enhancers for inhalation: correlation between *in vitro* and *in vivo* lung effects. *Int. J. Pharm.* 550 (1-2), 114–122. doi: 10.1016/j.ijpharm.2018.08.031

Sørli, J. B., Huang, Y., Da Silva, E., Hansen, J. S., Zuo, Y. Y., Frederiksen, M., et al. (2018b). Prediction of acute inhalation toxicity using *in vitro* lung surfactant inhibition. *ALTEX* 35 (1), 26–36. doi: 10.14573/altex.1705181

Swedish Work Environment Authority (2023). *The Swedish Work Environment Authority's Regulations and General Advice on Limit Values for Respiratory Exposure in the Work Environment*, 14. Stockholm.

Weinbruch, S., Scerri, M., Eduard, W., Thomassen, Y., Nordby, K. C., Berlinger, B., et al. (2023). Chemical composition of thoracic dust at workplaces during cement production. *Ann. Work Expo. Health* 67 (5), 609–621. doi: 10.1093/annweh/wxad011